

# Direct Aerosol Radiative Forcing Over Three Different Environments

T. Amaranatha Reddy, K. Krishna Reddy

**Abstract** - In the present report, we have utilised the inversion products of AERONET to study the aerosol optical properties and to estimate their direct radiative forcings over three different environments (Re Union, Nainital and Pune). Derived aerosol optical properties over all stations showed significant temporal (seasonal) and spatial variation. These properties have been used in SBDART model for the assessment of direct aerosol radiative forcing. The estimated averaged radiative forcings at top of the atmosphere are  $-2 \pm 1$ ,  $-7 \pm 4$  and  $-8 \pm 2 \text{ Wm}^{-2}$ , and the surface aerosol radiative forcings are  $-6 \pm 3$ ,  $-18 \pm 14$  and  $-36 \pm 8 \text{ Wm}^{-2}$  over Re Union, Nainital and Pune respectively. Subsequently the atmospheric forcings are  $3 \pm 2$ ,  $11 \pm 11$  and  $28 \pm 7 \text{ Wm}^{-2}$  over Re Union, Nainital and Pune respectively. Moreover, we found that higher the aerosol loading or aerosol optical depth the more aerosol radiative forcing. The estimated atmospheric aerosol radiative forcing will heat the lower atmosphere and leads modification of the thermal structure of the atmosphere. Hence, our study emphasized the importance of optical properties of aerosols in the estimation of direct aerosol radiative forcing.

**Keywords:** optical properties of aerosols; radiative transfer.

## I. INTRODUCTION

Atmospheric aerosols affect the climate directly by scattering and absorbing the incoming solar radiation as well as outgoing long wave radiation, and indirectly by modifying the cloud micro physical properties, cloud life time, etc. The effect of aerosols on climate is normally quantified in terms of radiative forcing and it depends on the optical properties, vertical structure of aerosols as well as the underlying reflecting surface (earth's surface or cloud albedo), etc (Marque et al., 2010). However, the induced radiative forcing due to the presence of aerosols in the atmosphere is not quantified well over the globe due to inadequate data sets on optical properties of aerosols. Estimation of aerosol optical properties over globally is difficult as they are high variable (composite, number concentration, size, etc of different species) in space and time and less life span. In order to understand the optical properties of aerosols there were many studies which focussed on seasonal variation of optical properties, size distributions, diurnal variations, vertical profiles, etc of aerosols over different environments (Dumka et al., 2006, Satheesh et al., 2008, Gadhavi and Jayaraman, 2010, Panicker et al., 2010, Srivastava et al., 2010, Sumit kumar et al., 2012, Samset et al., 2013). There were studies on aerosol radiative forcings over over different kinds of environments (Podgorny et al., 2001, Ramana et al., 2004, Satheesh et al., 2008, Gadhavi and Jayaraman, 2010, Panicker et al., 2010, Marcq et al., 2010).

**Revised Version Manuscript Received on December 26, 2015.**

T. Amaranatha Reddy, Department of Physics, Acharya Nagarjuna University, Guntur, India.

K. Krishna Reddy, Department of Physics, Yogi Vemana University, Kadapa, India.

Few studies were also concentrated on vertical distribution of aerosols over different regions (Satheesh et al., 2008, Hedge et al., 2009, Ramachandran et al., 2010). In the view of above the present study focussed on the characterisation of aerosols and to assess their radiative forcing over different kinds of environments like maritime (Re Union), clean (Nainital) and urban (Pune). Re Union Island ( $20^{\circ}88'N$ ,  $55^{\circ}48'E$ , 0 amsl) is in the South-Western Indian Ocean. This tiny (area:  $\sim 2500 \text{ km}^2$ ) holds two agglomerations with  $\sim 100,000$  inhabitants: Saint-Denis, located to the North and Saint-Pierre located to the South of it. The island has light/heavy industries, and large number of vehicles such as cars, trucks and buses operate with diesels which are the main sources of anthropogenic aerosols. The site also highly affected by sea spray via winds and a potential sea salt source over this area (Chatrapatty et al., 2001, Smirnov et al., 2009, Chatrapatty et al., 2013).

Nainital ( $29^{\circ}4'N$ ,  $79^{\circ}5'E$ , 1958 amsl) is a rural environment in the central Himalayan region. It is a high altitude station in the central Himalayan region in India and the station is free from industries around it, and a little number of automobiles that include buses, cars, and two wheelers are running in the city all of which will not significantly contribute to the production of aerosols. Being a high altitude location and free from local emission sources it provides important information on background changes of aerosol concentration, properties and its radiative effects (Sagar et al., 2004, Dumka et al., 2008). Pune ( $18^{\circ}53'$ ,  $73^{\circ}80'$ , 559 amsl) is an urban environment in the western part of an Indian continent. The site is an urban, densely populated and industrialized city in India. It has several small and large scale industries around it, and a large number of automobiles that include buses, cars, two wheelers and three wheelers are running in the city all of which contribute significantly to the production of aerosols (Panicker et al., 2010, Devara et al., 2015). Pune is highly influenced by local pollution as it is the urban environment whereas Nainital and Re Union are least affected by any major anthropogenic activities.

## II. INSTRUMENTATION AND METHODOLOGY

### 2.1. Instrumentation

The data presented in this paper were obtained by CIMEL Sun/sky radiometers attached with AERONET global network. It provides three primary products aerosol optical depth (AOD), perceptible water vapour content and inversion products obtained based on measured direct and diffuse radiation. The inversion products include physical, optical and radiative properties like size distribution, complex refractive index, asymmetry factor, single

scattering albedo etc. CIMEL sun-photometer measures the irradiance once for every 15 minutes centred at 340, 380, 440, 500, 675, 870, 940 and 1020 nm with a full width at half maximum of the 340 nm channel at 2 nm and the 380 nm filter at 4 nm, while the other channels with 10 nm. These solar irradiances are used to calculate optical and physical properties of aerosols. Rayleigh optical depth is subtracted out from the total optical depths to compute AOD at different wavelengths from direct sun irradiance, additionally ozone optical depth also removed in computation of AOD for 340, 500, 675 nm using climatologically mean values from London et al. (1976). A series of papers describes about instrumentation, measurements, accuracy and cloud screening procedure (Holben et al. 1998; Eck et al. 1999; Smirnov et al. 2000; Holben et al. 2001). In the data products, there are three levels of data quality available at AERONET. Level 1.0 contains unscreened data and it is considered as raw data without undergoing any processing. Level 1.5 contains the data which are cloud screened but not quality assured. This type of processed data is obtained from by removing the cloud influence on the unscreened data. The data from level 1.5 is further processed for quality to produce level 2.0 data. Level 2.0 contains the data which are both cloud screened and quality assured. In the present study it has been used level 2 data which is quality and cloud screened.

### 2.2. SBDART Model

The fluxes for aerosol and aerosol free cases were estimated using SBDART (Sanata Barbara DISORT Atmospheric Radiative Transfer) model (Ricchiuzzi et al., 1998). SBDART model is a tool that computes plane-parallel radiative transfer in clear/cloudy conditions within and at the surface of the earth's atmosphere. There were many scientific studies on aerosol radiative forcing and earth's radiation balance based on this model (Panicker et al., 2010, Ramachandran et al., 2010, Sumit Kumar et al., 2012). All the properties of aerosols that derived from inversion product of AERONET have been used as input parameters to the radiative transfer model to derive radiation flux.

### 2.3. Direct Aerosol Radiative Forcing

The Direct Aerosol Radiative Forcing (DARF) at any level in the atmosphere is defined as the difference between the clear-sky net shortwave radiative flux ( $F^A$ ) for the aerosol case and net shortwave radiative flux ( $F^C$ ) for the aerosol free atmosphere:

$$\Delta F = (F^{\downarrow A} - F^{\uparrow A}) - (F^{\downarrow C} - F^{\uparrow C}) \quad (1)$$

Arrows indicates the direction of the global fluxes:  $\downarrow$ = downward flux and  $\uparrow$ = upward flux. The instantaneous aerosol radiative forcing at top of the atmosphere (TOA) and bottom of the atmosphere (BOA) are calculated as following:

$$\Delta F_{TOA} = F^{\uparrow C} - F^{\uparrow A} \quad (2)$$

$$\Delta F_{BOA} = (F^{\downarrow A} - F^{\uparrow A}) - (F^{\downarrow C} - F^{\uparrow C}) \quad (3)$$

For the present work, the diurnal averaged direct aerosol radiative forcing values at surface, top of the atmosphere and in the atmosphere have been calculated. The details of analysis procedure and methodology are given elsewhere

(Ramana et al., 2004, Dumka et al., 2006, Panicker et al., 2010, Ramachandran et al., 2010, Sumit Kumar et al., 2012).

## III. RESULTS AND DISCUSSION

### 3.1. Optical properties of aerosols over different environments

#### 3.1.1. Aerosol optical depth

The temporal variations of monthly mean aerosol optical depth (AOD) at 441 nm in different environments has been shown in figure 1. The monthly mean AOD showed large variation over Re Union and it is varied from lowest value 0.03 to highest values 0.18 with an annual average of 0.07. The low AOD value is observed in the month of July and high value is observed in the month September. It is also observed that there is a 6 fold increment in AOD from July to September. As the site is a small island station and free from any major anthropogenic emissions most of the time the site affect mainly sea salt aerosols. From the figure it can be observed that large increment in AOD during September and September due to bio mass burning (Chatrapatty et al., 2001) where as during the other months the station is mainly affected by sea salt aerosols. As shown in figure 1, the monthly mean AOD showed large variation from lowest value 0.07 to highest values 0.58 with an annual average of 0.24 over Nainital. The low AOD values are observed in winter and post monsoon season, and high values are observed in summer monsoon seasons. It is also observed that there is an 8 fold increment in AOD from January to June. As the site is a high altitude station and free from any anthropogenic emissions most of the time the site is in the free troposphere and affect least by any anthropogenic activity. During winter due to shallow boundary layer most of the aerosols will not reach the station from distant sources. In this case the station will only be affected by the local pollutants which are very minute. This implies less aerosol concentration and gives lowest AOD in winter season. The high convective activity and frequent occurrence of dust storms are responsible for the higher AODs during June. Generally the AOD decreases during post monsoon season (September to October) due to rain washout and again from winter to summer the aerosol concentration increases. However there is gap in data points during monsoon season due to unavailable of solar radiation. The same type of variation in measured aerosol optical depths were also reported previously (Sagar et al., 2004). They have also observed six fold increments in AOD in June due to the long-range transport and local convection which lift up air mass from low altitude stations and bring subsequent horizontal transport.

The monthly mean AOD observed over Pune showed large seasonal variation and it is varied from lowest value 0.23 to highest values 0.68 with an annual average of 0.47 as shown in figure 1. The highest value and lowest value has been observed in January and June respectively. Local boundary layer dynamics associated with horizontal winds are mainly responsible for the variation of aerosol loading. The product of these two parameters gives the ventilation coefficient. In addition to the above emissions of pollutants and rainfall also causes the seasonal variation of AOD.

During winter the boundary layer height is very shallow and the magnitudes of horizontal wind also relatively less. This causes low ventilation coefficient leads to high aerosol loading by accumulation or trapping of aerosols. During summer monsoon period boundary layer height increases due to large surface heating and the magnitudes of horizontal wind also increases. This causes high ventilation coefficient leads to low aerosol loading by dispersing the aerosols. In addition to the above some of aerosols also will be washout by cloud scavenging and rain-washout process during monsoon period. So the both phenomenon reduce the aerosol loading over Pune during monsoon season (Ernest Raj et al., 1997). There are many studies that explain the role of ventilation coefficient in the trapping of aerosols over different sites (Krishnan and Kunikrishnan, 2004, Ramachandran et al., 2010). They also suggested that the boundary layer mixing height and associated with high (low) mean wind speed, the product of these two is measure of dispersion ability and called “ventilation coefficient”. Low ventilation coefficient allows more aerosols to accumulate in the lower atmospheric levels leads high surface concentrations though the column integrated concentrations are low and vice versa.

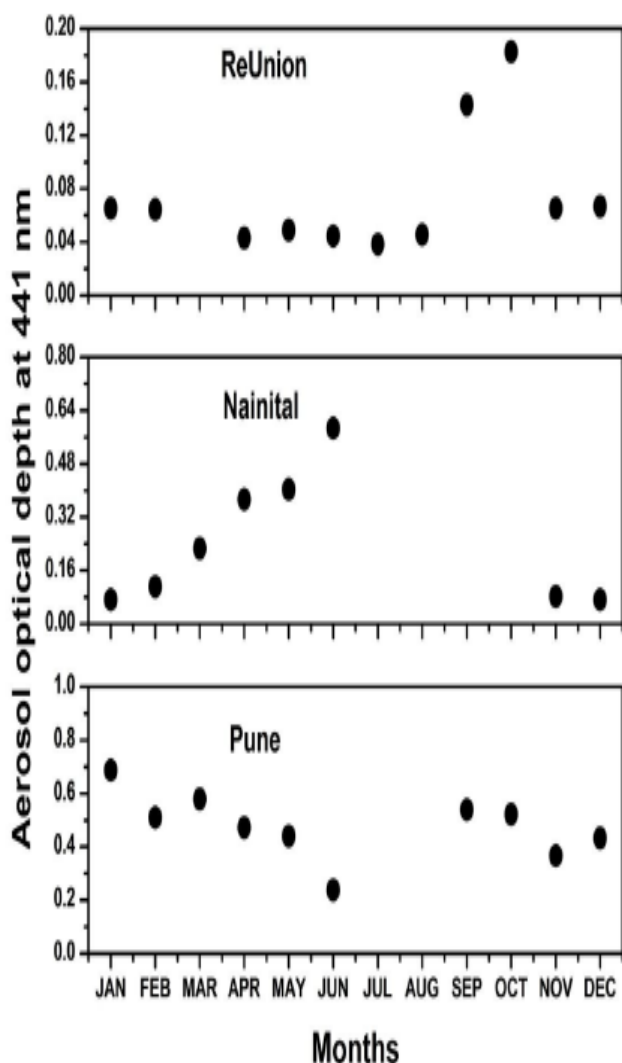


Figure 1: Temporal variations of monthly averaged of aerosol optical depth at 441 nm over three different environments during 2010.

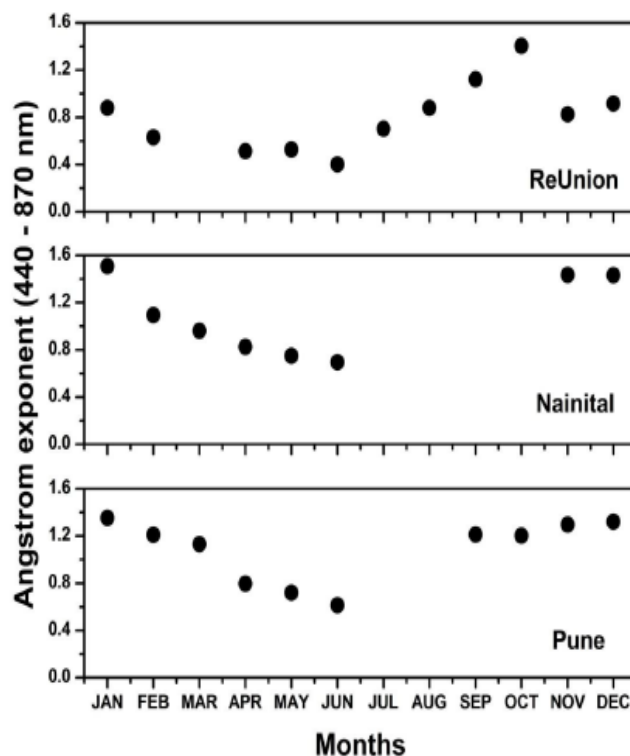


Figure 2: Temporal variations of monthly averaged Angstrom exponent (440 – 870 nm) over three different environments during 2010.

### 3.1.2. Angstrom exponent

Aerosol optical depths at different wavelengths contain information pertaining to their size distribution. A simple way of expressing the wavelength dependence of AOD is through the Angstrom relation (Angstrom 1964), expressed as:

$$\tau_{p\lambda} = \beta \lambda^{-\alpha} \quad (4)$$

where  $\tau_{p\lambda}$  is AOD at wavelength  $\lambda$ ,  $\alpha$  is Angstrom exponent,  $\beta$  is turbidity parameter. The Angstrom exponent  $\alpha$  is an index for the aerosol size distribution and depends on the ratio of the concentration of small (fine mode) to large (coarse mode) aerosols whereas  $\beta$  denotes the aerosol concentration present in the vertical column. Figure 2 shows the temporal variation of angstrom exponent over three different environments. The estimated  $\alpha$  in the present study ranges from nearly 0.4 to 1.4 with an average of 0.8 over Re Union. High and low alpha values were observed during October and June. The high values during October represent the domination of fine mode (mass burning) aerosols whereas low values during June represent the domination of coarse mode (sea salt) aerosols (Chatrapatty et al., 2001, Chatrapatty et al., 2013). The estimated alpha ranges from nearly 0.7 to 1.5 with an average of 1.0 over Nainital. High alpha values were observed during winter (November, December, January and February) whereas low values were found during summer monsoon (June). This high value of alpha could be mainly due to the bio mass burning during winter as most of the peoples use to burn the wood for getting warm. Previous studies on angstrom exponent also followed the same trend as shown in the present study (Sagara et al., 2004). The high alpha values during summer monsoon could be mainly due to long range transport of

mineral dusts (Sagar et al., 2004, Dumka et al., 2009, Hegde et al., 2009). The estimated angstrom exponent over Pune ranges from nearly 0.6 to 1.3 with an average of 1. High alpha values were observed during winter season (December, January and February) whereas low values were found during summer monsoon (June). The high values during winter represent the domination of fine mode aerosols whereas low values during summer monsoon represent the domination of coarse mode aerosols. This high value of alpha could be mainly due to the anthropogenic activities such as industrial pollution, vehicular emissions; etc produces high black carbon aerosols. Panicker et al (2010) showed that the contribution of black carbon aerosols total composite aerosols is high during winter whereas it is low during other seasons.

### 3.1.3. Single scattering albedo

Single scattering albedo is defined as the fraction of scattered radiation to the total extinction.

Single scattering albedo (SSA) = scattering/ extinction

Where extinction = scattering + absorption, the value of SSA can vary from 0 to 1 depending on properties of absorbing type aerosols. It is 0 if the extinction is caused by only absorption whereas 1 if the extinction is caused by only scattering. Figure 3 shows the temporal variation of Single scattering albedo over three different locations. It is varied from 0.83 to 0.96 at 439 nm with an average value 0.9 showing domination of scattered type aerosols over Re Union. The low values were found during January and February and highest values were found during October to December. The low value reveals the presence of relatively less scattered or high absorbing type aerosols and vice versa. The temporal variation of single scattering albedo over Nainital is varied from 0.83 to 0.98 with an average value of 0.92 at 439 nm represents relatively low absorbing type aerosols. This is mainly due to the absence of major anthropogenic activities over or near the site and the site also located on the hill and most of the times it will be in free troposphere (Sagar et al., 2004). The temporal variation of single scattering albedo varied from 0.86 to 0.89 at 439 nm over Pune. This represents relatively high absorbing type aerosols when compare to other two sites (Re Union and Nainital). The low values were found during winter and highest values were found during summer monsoon. The low value during winter reveals high fraction of black carbon aerosols to the total composite aerosols. The reported values of SSA and the seasonal variations are consistence with the previous studies (Panicker et al., 2010, Sumit Kumar et al., 2012). Panicker et al (2010) reported that the low values of SSA during winter obviously due to presence of high fraction of black carbon aerosols and they also reported that high SSA during summer monsoon. However these values were estimated by model with the help of aerosol optical depths at different wavelengths and black carbon measurements. Sumit Kumar et al (2012) also reported the same trend with minimum SSA during winter and maximum SSA during summer monsoon.

### 3.1.4. Asymmetry factor

The asymmetry factor ( $g$ ) indicates the strength of forward scattering and it varies between 0 and 1. For total forward scattering the asymmetry factor is 1 where as for total backward scattering it is 0. The scattering of the light by aerosols can be derived from Mie theory. If the size of the particle is higher than the wavelength of interacting radiation, most of the radiation will get scattered in forward direction and vice versa. It can also be observed the same asymmetry factor at all wavelengths when the size of the particle is much higher than the wavelength band. The asymmetry factor varies with wavelength when the sizes of aerosols are comparable with wavelength band of interacting radiation. Figure 4 shows the temporal variation of asymmetry factor over three different locations. It is varied from 0.7 to 0.76 at 439 nm over Re Union showing most of the scattered radiation in forward direction. The low values were found during winter (April to October) and highest values were found during summer (November to March). The low value during winter reveals the less forward scattering where as high values during monsoon reveals the high forward scattering. It is also observed that the asymmetry factor at all wavelengths (679, 872 and 1020 nm) are equal except at 439 nm for all the months. This gives clue on bimodal size distribution of aerosols with minimum deviation in both modes. The sizes of coarse mode particles are much higher than the wavelength band of 679 – 1020 nm which reveals the sea salt particles and there is negligible variation in asymmetry factor. The sizes of fine mode aerosols are in between or nearly comparable with 439 nm and this could be the reason for variation of asymmetry factor at lower and higher wavelengths. Previous report shows the concentration of fine mode aerosols are almost same during December to June and they increase by almost factor ~ 2 during August to November (Chatrapatty et al., 2001). The same parameter is increased by factor ~ 3 during night times. This may be the reason for the variation of asymmetry factor at different wavelengths.

The temporal variation of asymmetry factor is varied from 0.67 to 0.72 at 439 nm over Nainital. The low values were found during winter and highest values were found during monsoon (June), and these values decreased as reaching the post monsoon. The low value during winter reveals the less forward scattering where as high values during monsoon reveals the high forward scattering. From the figure it can be observed that the asymmetry factor at all wavelengths (439, 679, 872 and 1020 nm) are different during winter and these values were attained same values as reaching the monsoon season. From this observation, it can be concluding that the sizes of aerosols are higher when comparing to the wavelength band of radiation (439 – 1020 nm) during monsoon. This may be due to the size growth of aerosols with water vapour content as the atmosphere contains hygroscopic aerosol. As water vapour content reaches maximum during June the aerosols grow in size by attracting or condensing the water vapour on them. Previous reports show the increment of size of aerosols from winter to monsoon season over the same location (Sagar et al., 2004, Dumka et al., 2006).

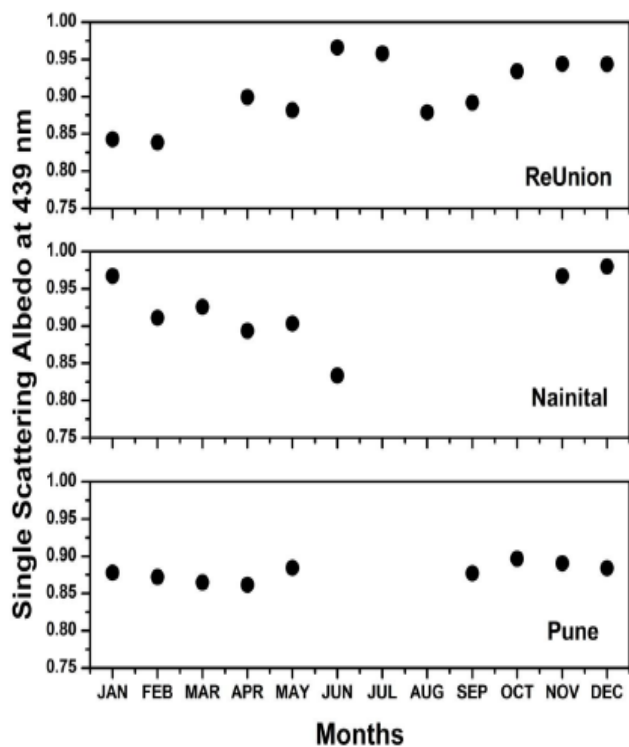


Figure 3: Temporal variations of monthly averaged of single scattering albedo (SSA) over three different environments during 2010.

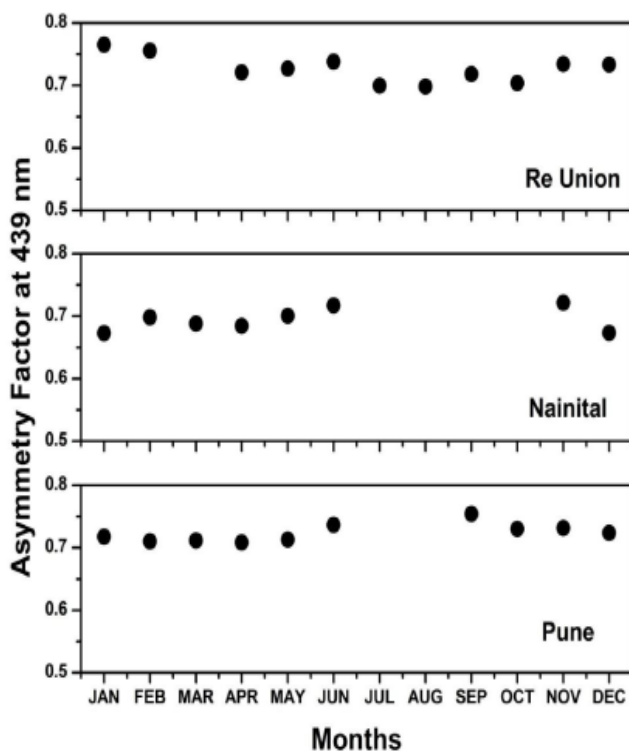


Figure 4: Temporal variations of monthly averaged of asymmetry factor over three different environments during 2010.

The temporal variation of asymmetry factor over Pune is varied from 0.7 to 0.75 at 439 nm showing most of the scattered radiation in forward direction. The temporal variation is high at both wavelengths when compare to Re Union and Nainital. The low values were found during winter and highest values were found during monsoon

(June), and these values decreased as reaching the post monsoon. The low value during winter reveals the less forward scattering where as high values during monsoon reveals the high forward scattering. It is also observed that the asymmetry factor at all wavelengths (439, 679, 872 and 1020 nm) are different during winter and these values were attained same values as reaching the monsoon season. From this observation, it can be concluding that the sizes of aerosols are higher when comparing to the wavelength band of radiation (439 – 1020 nm) during monsoon season. The variation in asymmetry factor at different wavelengths during winter reveals the huge size range of aerosols. Previous reports show the increment of size of aerosols from winter to summer monsoon season over the different locations in Indian continent (Sagar et al., 2004, Ramachandran et al., 2010, Gadavi and Jayaraman, 2010).

#### IV. DIRECT AEROSOL RADIATIVE FORCING OVER DIFFERENT ENVIRONMENTS

In the present study, we have estimated aerosol radiative forcing over three different kinds of environments like maritime (Re Union), clean (Nainital) and urban (Pune). Derived aerosol optical properties such as aerosol optical depth, single scattering albedo and asymmetry factor at different wavelengths, and water vapour content, etc by AERONET inversion have been used in the SBDART model to obtain radiation flux in the case of aerosols. Default (exponential) vertical profiles of aerosol extinction and other parameters such latitude, longitude also used. For the clear picture on spatial and temporal (seasonal) variation of radiative forcing, we estimated the modelled forcing for all months from January – Dec 2010. Figure 5 depicts the estimated monthly averaged aerosol radiative forcing at TOA (Top of Atmosphere), BOA (Bottom of Atmosphere) and AF (Atmospheric Forcing) over Re Union, Nainital and Pune. Figure 5 shows temporal variations of monthly averaged direct aerosol radiative forcing at TOA (Top of Atmosphere), BOA (Bottom of Atmosphere) and AF (Atmospheric Forcing) over three different environments during 2010. Figure clearly shows that monthly averaged surface forcing values increased from summer (January) and reaches comparatively maximum values in winter (October) over Re Union. Again these values shows decreased when reaching the summer (December) with low surface forcing values. The high surface radiative forcing  $\sim -13 \text{ Wm}^{-2}$  during October is because of aerosol loading in the atmosphere primary due to fires occurring in the south and east Africa (Chatrapatty et al., 2001). Low values of surface radiative forcing  $\sim -3 \text{ Wm}^{-2}$  during December to April is mainly due to washout of aerosols during post monsoon season over the observational site (Ogren et al., 1984, Chatrapatty et al., 2001). During this season, there is intense rainfall in tropical regions, which mainly contribute to aerosol removal processes via scavenging processes. It has also been derived aerosol radiative forcing at the top of the atmosphere and the difference between the top of the atmosphere and surface forcing is considered as atmospheric forcing, which varied from  $\sim +7 \text{ Wm}^{-2}$  to  $+1 \text{ Wm}^{-2}$  and these values also followed the same trend as surface radiative forcing. Monthly averaged surface forcing values

## Direct Aerosol Radiative Forcing Over Three Different Environments

have shown increasing trend from winter (January) and reaches comparatively maximum values in summer monsoon (June) over Nainital. The high surface radiative forcing  $\sim -40 \text{ Wm}^{-2}$  during June is because of aerosol loading in the atmosphere due to long range transport of mineral and other aerosols. Low values of surface radiative forcing  $\sim -4 \text{ Wm}^{-2}$  during November and December is mainly due to washout of aerosols during post monsoon season over the observational site (Sagar et al., 2004; Hegde et al., 2009). Subsequently atmospheric forcing varied from  $\sim +33 \text{ Wm}^{-2}$  to  $+0.8 \text{ Wm}^{-2}$  and these values also followed the same trend as surface radiative forcing. The estimated atmospheric aerosol radiative forcing values over Nainital followed the similar trend as other locations like Bangalore and Gadanki but the magnitudes are low when compare to other low altitude stations such as Bangalore and Gadanki (Satheesh et al., 2008; Gadavi and Jayaraman 2010). This is mainly due to low concentration of aerosols, especially absorbing type aerosols such as black carbon as the site is a high altitude location and it is situated far away from any major anthropogenic activities. As shown in figure 5 the monthly averaged surface forcing values decreased from winter (January) to summer monsoon (June) over Pune. Again these values increased when reaching the post monsoon season (September) with high surface forcing value. The high surface radiative forcing  $\sim -46 \text{ Wm}^{-2}$  during January is because of high accumulation of aerosols in the atmosphere due to low mixing height associated with low winds (the product of these two gives ventilation coefficient). Low values of surface radiative forcing  $\sim -21 \text{ Wm}^{-2}$  during June is mainly due to dispersion of aerosols in the atmosphere and washout of aerosols during monsoon season over the observational site. Subsequent atmospheric forcing varied from  $\sim +39 \text{ Wm}^{-2}$  to  $+18 \text{ Wm}^{-2}$  and these values also followed the same trend as surface radiative forcing. The estimated atmospheric aerosol radiative forcing values over Pune is followed the similar trend as other urban locations like Ahmedabad with different magnitudes (Ramachandran et al., 2010). The low values of radiative forcings in the atmosphere during monsoon could be due to wash out of aerosols. Previously it has been shown that a decrease of approximately 36% of aerosol contribution to the atmosphere from pre monsoon to monsoon season and this is directly related to the amount of rain fall received over the site (Ernest raj et al., 1997). They also concluded that the effect has not changed whatever be the increase in aerosol loading.

The estimated annual atmospheric forcing due to aerosols are  $3 \pm 2 \text{ Wm}^{-2}$ ,  $11 \pm 11 \text{ Wm}^{-2}$  and  $28 \pm 7 \text{ Wm}^{-2}$  over

Re Union, Nainital and Pune respectively. Magnitude of the standard deviation is very high approximately equals to the mean value over Nainital, it is about 75% of mean value over Re Union and it only about 25% over Pune. The site, Re Union is an island and most of the time it is influenced by sea salt aerosols which are scattering type aerosols. It also slightly influenced by biomass burning during winter seasons which produces absorbing type aerosols. The combination of these two effects gives relatively less radiative forcing in the atmosphere. The site, Nainital is a high altitude station and is free from any major anthropogenic activities which provides background aerosols most of the time. It also slightly influenced by biomass burning and long range transport of aerosols from far-off regions. The combination of these two effects gives relatively moderate radiative forcing in the atmosphere. High value of radiative forcing represents high absorbing type aerosols or loading of aerosols over Pune. The site, Pune is an urban and it is highly influenced by many anthropogenic activities such as industrial emissions, vehicular emissions and etc. These activities produce high concentration of absorbing type aerosols gives relatively high radiative forcing in the atmosphere when compare to other two sites. Apart from the variation of magnitude of aerosol radiative forcing in the atmosphere, it is also seen that there is large variation in standard deviation. This large deviation shows the wide range of aerosol loading during a year over Nainital and Re Union where as the low deviation represents less variability of aerosol loading over Pune. The magnitude of standard deviation gives not only gives clue about variability of aerosol loading it also gives the ventilation coefficient and effective removal process of aerosols. From the magnitudes of mean and standard deviation of aerosol radiative forcing it can be concluded that the concentration of aerosols not only varies with the location but also varies with time. The estimated radiative forcing in the atmosphere will heats the lower atmosphere relative to the surface have been demonstrated to be able to interact with dynamical processes in various scales to alter atmospheric circulation, clouds and precipitation (Koch et al., 2010; Chien Wang, 2013). If the warming of the atmosphere is high when compare to the surface will reduce the upward movement of moisture air and hence reductions of cloud cover (Ackerman et al., 2000). The forcing can also change the local boundary layer characteristics, hydrological cycle by reducing the surface reaching solar radiation (Ramanathan et al., 2001).

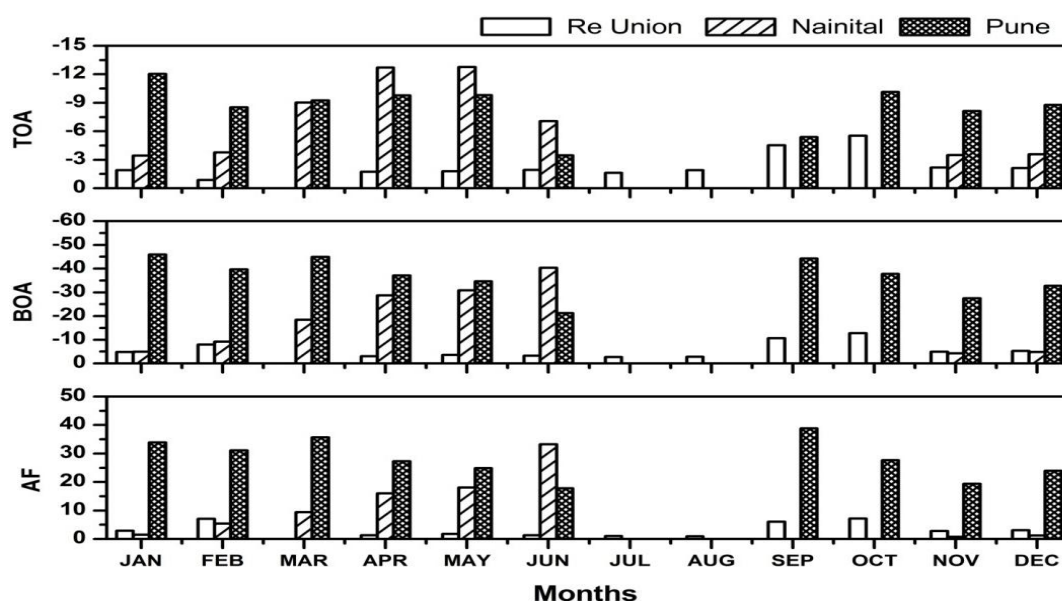


Figure 5: Estimated monthly averaged direct aerosol radiative forcing at TOA (Top of Atmosphere), BOA (Bottom of Atmosphere) and AF (Atmospheric Forcing) over three different environments during 2010.

## V. SUMMERY

Direct aerosol radiative forcings were estimated over three different kinds of environments like maritime (Re Union), clean (Nainital) and urban (Pune). The derived aerosol optical properties by AERONET inversion have been used in the SBDART model to obtain radiation flux in the case of aerosols. Monthly averaged surface radiative forcing values showed large temporal variation over all the locations. The estimated annual aerosol radiative forcings at surface were  $-6 \pm 3 \text{ Wm}^{-2}$ ,  $-18 \pm 14 \text{ Wm}^{-2}$  and  $-36 \pm 8 \text{ Wm}^{-2}$  and subsequently the atmospheric forcings were  $3 \pm 2 \text{ Wm}^{-2}$ ,  $11 \pm 11 \text{ Wm}^{-2}$  and  $28 \pm 7 \text{ Wm}^{-2}$  over Re Union, Nainital and Pune respectively. The estimated radiative forcing in the atmosphere will heats the lower atmosphere relative to the surface have been demonstrated to be able to interact with dynamical processes in various scales to alter atmospheric circulation and precipitation. If the warming of the atmosphere is high when compare to the surface will reduce the upward movement of moisture air and hence reductions of cloud cover.

## ACKNOWLEDGMENTS

The authors are thankful to NASA for the AERONET project (<http://aeronet.gsfc.nasa.gov/>) for providing data for the present work. The data are downloaded from the AERONET inversion products.

## REFERENCES

1. ACKERMAN, A. S., TOON, O. B., STEVENS, D. E., HEYMSFIELD, A.J., RAMANATHAN, V., and WELTON, E.J., 2000, Reduction of tropical cloudiness by soot. *Science*, **288**(5468), pp. 1042-1047.
2. ANGSTROM A., 1964. The parameters of atmospheric turbidity. *Tellus*. **16**: 64–75.
3. CHATRAPATTY, BHUGWANT., EMMANUEL RIVIERE, PHILIPPE KECKHUT and JEAN LEVEAU., 2001, Variability of carbonaceous aerosols, ozone and radon at Piton Textor, a mountain site on Re'union island (south-western Indian Ocean), *Tellus*, **53B**, 546–563.
4. CHATRAPATTY, B., MILOUD, B., OLIVIER, F., LAURA, C., BRUNO, S., EVA, L., 2013, High Contribution of Sea Salt Aerosols on Atmospheric Particles Measured at an Urban Tropical Location in Reunion Island, *Journal of Environmental Protection*, 2013, 4, 828-842.
5. CHIEN, WANG., 2013, Impact of anthropogenic absorbing aerosols on clouds and precipitation: A review of recent progresses. *Atmospheric Research*, **122**, 237–249.
6. DEVARA, P. C. S., VIJAYA KUMAR, K., PRAMOD, D., SAFAL, M., RAJU, P., RAO, P. S. P, Celebration-induced air quality over a tropical urban station, Pune, India, *Atmospheric Pollution Research*, **6**, 511-520
7. DUMKA, U. C., SATHEESH, S. K., PANT, P., HEGDE, P., and KRISHNA MOORTHY, K., 2006, Surface changes in solar irradiance due to aerosols over central Himalayas. *Geophysical Research Letters*, **33**, L20809; doi: 10.1029/2006GL027814.
8. DUMKA,, U.C., MOORTHY, K. KRISHNA., SATHEESH, S. K., SAGAR, R., and PANT, P., 2008. Short- Period Modulations in Aerosol Optical Depths over Central Himalayas: Role of Mesoscale Processes. *J. Climate Appl. Meteor.* **47**: 1467-1475.
9. DUMKA, U. C., SAGAR, R., PANT, P., 2009, Retrieval of Columnar Aerosol Size Distributions from Spectral Attenuation Measurements over Central Himalayas. *Aerosol and Air Quality Research*, **9**, pp. 344-351.
10. ECK, T.F., B.N. HOLBEN., J.S. REID., O. DUBOVIK., A. SMIMOV., N.T. O'NEILL., I. SLUTSKERA., and S. KINNE., 1999. Wavelength dependence of the optical depth of biomass burning, urban, and desert dust aerosols. *J. Geophys. Res.*, **104**, 31,333-31,349.
11. ERNEST RAJ, P., DEVARA, P C S., MAHESH KUMAR, R S., PANDITHURAI, G DHANI, K K., 1997, Lidar measurements of aerosol column content in an urban nocturnal boundary layer, *J. Atmospheric Research*, **45**, 201 – 216.
12. GADHAVI, H. and JAYARAMAN, A., 2010, Absorbing aerosol: contribution of biomass burning and implications for radiative forcing. *Journal of Annales Geophysicae*, **28**, pp. 103-111.
13. HEGDE, P., PANT, P. and BHVANI KUMAR, Y., 2009, An integrated analysis of Lidar observations in association with optical properties of aerosols from a high altitude location in central Himalayas. *Atmospheric Science Letters*, **10**, pp. 48–57.
14. HOLBEN, B.N., et al. (1998). AERONET - A federated instrument network and data archive for aerosol characterization. *Remote Sens. Environ.*, **66**, 1-16.
15. HOLBEN, B. N., et al. (2001). An emerging ground-based aerosol climatology: Aerosol optical depth from AERONET. *J. Geophys. Res.*, **106**, 12,067– 12,097.
16. KRISHNA, P., KUNHIKRISHNAN, P. K., 2004. Temporal variations of ventilation coefficient at a tropical Indian station using UHF wind profiler. *Current Science*, **86**, No. 3.

17. KOCH, D., DEL GENIO, A. D., 2010. Black carbon semi-direct effects on cloud cover: review and synthesis. *Atmospheric Chemistry and Physics*, **10**, 7685–7696.
18. LONDON, J., R. D. BOJKOV., S. OLTMANS., and J. I. KELLEY., 1976. Atlas of the global distribution of total ozone July 1957-June 1967, NCAR Tech. Note 133 STR, 276 pp., Natl Cent for Atmos. Res., Boulder, Colo.
19. MARCQ, S., LAJ, P., ROGER, J.C., VILLANI, P., SELLEGRI, K., BONASONI, P., MARINONI, P., CRISTOFANELLI, P., VERZA, G.P. and BERGIN, M., 2010, Optical properties and radiative forcing in the high Himalaya based on measurements at the Nepal Climate Observatory-Pyramid site (5079 m.a.s.l.). *Atmospheric Chemistry and Physics*, **10**, pp. 5859–5872.
20. OGREN, J. A., GROBLICKI, P. J., and CHARLSON, R. J., 1984. Measurement of the removal rate of elemental carbon from the atmosphere. *Sci. Total Environ.* **36**, 329–338.
21. PANICKER, A. S., PANDITHURAI, G., SAFAI, P. D., DIPU, S., DONG-I, LEE., 2010. On the contribution of black carbon to the composite aerosol radiative forcing over an urban environment. *Journal of Atmospheric Environment*, **44**, 3066-3070.
22. PODOGORNY and RAMANATHAN, V., 2001, A modelling study of the direct effect of aerosols over the tropical Indian Ocean. *Journal of Geophysical Research*, **106**, 24, 097-24,105.
23. RAMACHANDRAN, S., SUMITA, K., 2010. Black carbon aerosols over an urban region: Radiative forcing and climate impact. *Journal of Geophysical Research*, **115**, D10202. doi:10.1029/2009JD013560.
24. RAMANA, M.V., RAMANATHAN, V. and PODGORNY, I.A., 2004, The direct observations of large aerosol radiative forcing in the Himalayan region. *Geophysical Research Letters*, **31**, L05111, doi: 10.1029/2003GL018824.
25. RAMANATHAN, V., CRUTZEN, P. J., KIEHL, J. T., and ROSENFELD, D., 2001, Aerosols, Climate, and the hydrological cycle, *Science*, **294**, 2119– 2124.
26. RICCHIAZZI, P., YANG, S., GAUTIER, C. and SOWLE, D., 1998, SBDART, A research and teaching tool for plane-parallel radiative transfer in the Earth's atmosphere. *Bulletin of the American Meteorological Society*, **79**, pp. 2101–2114.
27. SAGAR, R., KUMAR, B., DUMKA, U. C., MOORTHY, K. K., and PANT, P., 2004, Characteristics of aerosol spectral optical depths over Manora Peak: A high altitude station in the central Himalayas. *Journal of Geophysical Research*, **109**, D06207: doi: 10.1029/2003JD003954.
28. SAMSET, B.H., MYHRE, G., SCHULZ, M., BALKANSKI, Y., BAUER, S., BERNTSEN, T.K., BIAN, H., BELLOUIN, N., DIEHL, T., EASTER, R.C., GHAN, S.J., IVERSEN, T., KINNE, S., KIRKEVAG, A., LAMARQUE, J.-F., LIN, G., LIU, X., PENNER, J.E., SELAND, O., SKEIE, R.B., STIER, P., TAKEMURA, T., TSIGARIDIS, K. and ZHANG, K., 2013, Black carbon vertical profiles strongly affect its radiative forcing uncertainty. *Atmospheric Chemistry and Physics*, **13**, pp. 2423–2434.
29. SATHEESH, S.K., MOORTHY, K.K., BABU, S.S., VINOJ, V. and DUTT, C.B.S., 2008, Climate implications of large warming by elevated aerosol over India. *Geophysical Research Letters*, **35**, L19809, doi: 10.1029/2008GL034944.
30. SMIRNOV, A., B.N. HOLBEN., T.F. ECK., O. DUBOVIK., and I. SLUTSKER., 2000. Cloud screening and quality control algorithms for the AERONET data base, *Remote Sens. Environ*, **73**, 337-349.
31. SMIRNOV, A., et al., 2009, Maritime Aerosol Network as a component of Aerosol Robotic Network, *J. Geophysical Research*, **114**, D06204, doi:10.1029/2008JD011257.
32. SRIVASTAVA, A. K., PANT, P., HEGDE, P., SINGH, SACHIDANAND., DUMKA, U. C., NAJA, MANISH., SINGH, N., and BHAVANI KUMAR, Y., 2010, Influence of south asian dust storm on aerosol radiative forcing at high-altitude station in central Himalayas. *International Journal of Remote Sensing*, **32**, pp. 7827-7845.
33. SUMIT, KUMAR., DEVARA, P.C.S., 2012, Aerosol characterization: comparison between measured and modelled surface radiative forcing over Bay of Bengal. *Remote Sensing Letters*, **3**, pp. 373–381.